Hardware Simulator Models and Methodologies for Controlled Indoor Performance Assessment of High Sensitivity AGPS Receivers

Gérard Lachapelle
Department of Geomatics Engineering
University of Calgary
2500 University Drive NW
Calgary, Alberta T2N 1N4, Canada
Lachapelle@geomatics.ucalgary.ca

Co-Authors
Elizabeth Cannon, Richard Klukas, Sanjeet Singh, Robert Watson University of Calgary
Peter Boulton, Arnie Read, Ken Jones, Spirent Communications, UK

1 Abstract

High sensitivity GPS-enabled mobile telephones and personal digital assistants are being introduced for emergency call location and location-based commercial services. Simulation of weak GPS signals received in various environments has been proposed as a cost-efficient method of verifying the positioning performance of such mobile telephones. Recent results (e.g. Boulton et al 2002) have demonstrated both the success and limitations of weak signal and multipath models implemented in an advanced GPS hardware simulator. In particular, the lack of variability of multipath delay as a function of time is suspected to be a major reason for the discrepancy between simulator and field test results. This paper discusses how these model limitations have been recently addressed and demonstrates the improvement in the correlation between the simulator results and field test results. A high sensitivity GPS receiver type is used to collect data under two scenarios, namely one in an outdoor environment near a building and another inside a residence. This data is then used as a baseline to attempt to generate signals in the simulator that results in measurements with similar stochastic characteristics. An analysis of the results in terms of fade and position demonstrates the viability of this approach to test receivers under controlled environments.

2 Introduction

Assisted-GPS technology is used to acquire and track weak signals in partly or totally obscured locations, such as in urban canyons and indoors. External assistance consists of ephemeris and Doppler information used during the acquisition phase. Since the largest user group by far is cellular phone users, the external information coming from a GPS reference receiver is usually provided to the receiver via the cellular phone network. Once signal acquisition has occurred, successful weak signal tracking is achieved through the use of longer signal integration time periods (e.g. Garin et al 1999). A receiver capable of tracking weak signals is referred to as a high sensitivity GPS (HSGPS) receiver herein. In order to test the HS capability of an AGPS receiver, signals can first be acquired under normal LOS conditions in the field or on a simulator and then the receive can be moved indoor in the case of field testing or the signals modified in the case of a simulator.

GPS hardware simulators can accurately replicate signals-in-space through modeling of the satellite constellation motion and that of the user. In a live field environment, the GPS receiver, typically embedded in a cellular phone handset, is subject to the effects of signal degradation caused by path loss [the attenuation of the line-of-sight (LOS) signal as it propagates from satellite to user and, in particular, multipath or reflected signals. For a laboratory test to serve satisfactorily as an alternative to field tests in weak GPS signal environments, the modeling of this

signal degradation and of the suboptimal location environments (e.g., urban canyon and indoor) must be truly representative. In addition, tests must be conducted at numerous simulated locations, each of which can be essentially regarded as having a randomly distributed multipath environment. In this paper, the Spirent GSS 6560 GPS RF simulator, that has the capability to model weak signal environments through an advanced multipath model implemented in the Spirent SimGEN software, is used to assess its ability to reproduce such environments.

The multipath model initially used in the GSS 6560 employed a random but fixed delay for the multipath echoes (Boulton et al 2002, Cannon et al 2003). This had some limitations when applied to High Sensitivity (HS) GPS data collected in a weak signal environment such that the simulator data was not fully representative of field conditions. “Representative” data is defined here as data that has similar stochastic and spectral characteristics, since no attempt is made to reproduce a specific environment but rather an “equivalent” environment. Spirent has since extended its multipath model to include a variable delay component that takes satellite elevation and azimuth into account. The model is described in the next section.

The methodology used herein consists of collecting field measurements in selected representative environments with an HSGPS receiver, estimating associated signal fading and code noise and multipath, and attempting to reproduce the “stochastic” conditions encountered with the same receiver tracking simulator-generated signals instead. Two environments are used in this paper, namely a building-shaded outdoor location and an indoor environment represented by a North American wood-structure private residence.

3 GSS 6560 Variable Delay Multipath Model

The multipath model used initially was derived in the context of conducting many hundreds of tests in rapid succession in order to minimise the time taken to fully assess receiver performance in diverse locations and environments. These would be representative of a real cellular phone call distribution model, with appropriate percentages of emergency calls from rural, suburban and highway, for example. In such circumstances, the phone is required to provide an almost instantaneous position response and hence the need to model variation of gradual environmental degradation of the GPS signals is not as strong, with the obvious exception of modelling amplitude fading and level noise. The original model, therefore, employed a random but fixed delay for the multipath echoes generated.

However, early experiments involved capturing performance over a more extended period when compared with the GPS receiver validation test cases (Boulton et al 2002). The argument for having a fixed echo delay is therefore much diminished in this more general testing case. Spirent therefore undertook to extend the model to include a variable delay component. The initial assumptions were as follows:

1) Each multipath signal can be associated with a single signal reflection source, which would typically be a regularly shaped building with vertical sides.
2) The reflection surface may be viewed as a vertical, regular plane, such that signal reflection is uniform in all directions.
3) The signal source is so remote that incident angles are effectively the same at all points in the immediate vicinity.

It can be readily shown that for a reflected signal received at a point located in front of a reflecting surface (see Figure 1), the total additional path length, δ, due to signal delay is given by

$$\delta = 2D \cos\theta \qquad (1)$$

where D is the distance from the receiving antenna to the reflector. The distance, S, to the point of reflection is given by:

$$S = D / \cos\theta. \qquad (2)$$

Reflection may occur in any plane, not just in the local vertical or horizontal plane, so one needs to know the orientation of the satellite's LOS in relation to the reflecting surface. The direction of the satellite's LOS is usually expressed in terms of its elevation and azimuth angles in the local geodetic frame. Relating this to the reflection surface is not a problem for satellite elevation, ε, since we have already assumed that the reflecting plane is orthogonal to the local horizontal plane. However, the relationship is undefined for the satellite azimuth. A method for initialising this angle, α_i, is needed so that a representative value for θ may be determined using the relationship

$$\cos(\theta_i) = \cos(\varepsilon_i).\cos(\alpha_i). \tag{3}$$

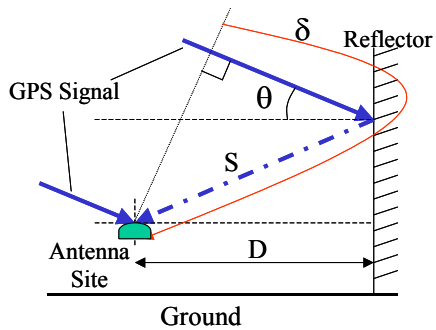

Figure 1: Signal reflection

In the original model the initial value for the additional path, δ_i, was determined randomly from an exponential distribution. This does not directly translate to a distance from the reflecting surface, so to some extent θ and D may be determined arbitrarily, but with some boundary conditions applied. For a given value of δ we can determine a range of values for which the reflector distance, D, is valid. From (1) we have

$$D = \delta_i/2\cos(\theta_i).$$

This is a minimum when $\theta = 0$ but from (3) θ cannot be less than ε, so D_{min}, the minimum possible distance from the reflection surface, is given by

$$D_{min} = \delta_i/2\cos(\varepsilon_i) \tag{4}$$

To find the equivalent D_{max} we assume that the maximum delay path, δ_{max}, specified by the user, is double the maximum distance to the reflection point, or

$$S_{max} = \delta max/2$$

From (2) we obtain

$$D_{max} = \delta_{max}.\cos(\varepsilon_i)/2. \tag{5}$$

δ_{max} must, of course, have been originally set by the user to be consistent with the mean delay value used to specify the original exponential distribution. For valid geometry, $D_{min} < D_{max}$ and using (4) and (5) this gives

$$\delta_i < \delta_{max}.\cos^2(\varepsilon_i) \tag{6}$$

During the actual simulation δ, D and α must be continuously determined. δ_i is generated from the exponential as before but within the constraint of (6). For D, we need to choose at random a value between valid upper and lower bounds. Equation (4) can be used again to determine the

minimum possible distance, D_1. Equation (5) will not yield the required answer for the upper bound, D_2, however, as it uses δ_{max} rather than δ_i. From equations (1) and (2)

$$D_2^2 = \delta_i.S/2.$$

If we limit S to $\delta_{max}/2$ then

$$D_2 = 0.5\sqrt{(\delta_i\delta_{max})}. \quad (7)$$

D may now be randomly selected by the model to be within the range D_1 to D_2. This value of D subsequently remains fixed throughout the lifetime of the multipath signal. The values for D and δ_i are now used in (1) to determine the initial reflection angle, θ_i, and thereafter the initial azimuth angle with respect to the reflecting surface, α_i, using (2).

All subsequent calculations of multipath distance and hence delay are derived from equation (1), with θ determined by (3), where ε_i becomes the current satellite elevation, and α_i becomes the sum of its initial value and the change in satellite azimuth with respect to the local geodetic frame since this reflection was initialised. Note that the boundary condition

$$D/\cos(\theta) <= \delta_{max}/2$$

must be applied to ensure that the reflection path length does not exceed the allowed limit. If it does then the multipath signal is considered invalid because the reflection is too distant, and it is replaced by a new valid condition. In this case the reflection is not interrupted, but an appropriate step in pseudorange is applied.

It is assumed throughout that no change in simulated vehicle position occurs during the test. Future work may involve modelling the changing distance between the vehicle and the reflecting surface. However, it would also be necessary to then consider switching between different reflectors when the separation becomes too large or too small.

In the simulator, one of four potential categories for each satellite can be selected, namely

Cat A: Satellites are not simulated - totally obscured
Cat B: LOS transmission occurs – no obscuration
Cat C: LOS transmission plus reflections (echoes)
Cat D: Reflected transmission (echoes only)

The Spirent GSS 6560 is a 12-channel simulator. As such, a total of 12, satellite, LOS and echo signals may be simulated. After categorization of each satellite, the 12 simulator channels must be allocated to the LOS and echo signals that are to be simulated. The channel allocation algorithm used in the GSS 6560 assumes that the number of simulator channels will generally be more than the number of unobstructed satellites. Therefore, at least a LOS signal will be simulated for each visible satellite. A second assumption made is that lower elevation satellites will in practice generate more echoes. Details of the channel allocation algorithm may be found in Boulton et al (2002). The SimGEN software uses the U.S. Coast Guard Almanac information to generate the GPS constellation for the time and location of the simulation. The default received satellite power was used. This power level is 10 dB above the minimum received level.

4 Outdoor Shaded Signal Environment Testing

A representative 20-minute sample was chosen from a 6-hour field test performed on the University of Calgary campus on 4 July 2002. This data set was also used by Boulton et al (2002) to test the initial GSS 6560 simulator model. A HSGPS SiRF STARIIe receiver and NovAtel 600 antenna were used at the remote site. The test was conducted in differential mode to eliminate satellite and atmospheric effects. A NovAtel OEM4 receiver system was used at the reference

station located less than 200 m away. The surrounding signal shading geometry at the remote site is shown in Figure 2. Fading values were calculated by differencing the C/N_o values between the reference and remote receivers (MacGougan 2003). The SiRF receiver tracked eight satellites during the interval selected. However, as the GSS 6560 simulator owned by the University of Calgary has 12 channels and two channels were used for echo signal generation, two of the satellites with the most sporadic tracking were removed from the signal simulation part to ensure valid comparison. Of the remaining six satellites tracked, PRN 22 provide echo-only signals due to shading and PRN 18 was obscured by coniferous tree shading, as shown in Figure 2. These two satellites are therefore particularly suitable to test the simulator's ability to reproduce signals with equivalent characteristics. The estimated pseudorange errors for the satellites tracked during the 20-minute sample period are shown in Figure 2 and reach 50 m RMS. There errors are caused by a combination of high noise due to fading and multipath. Since these are single differenced measurements using a high performance receiver at the reference stations, over 90% of the above errors are caused by a combination of these two effects.

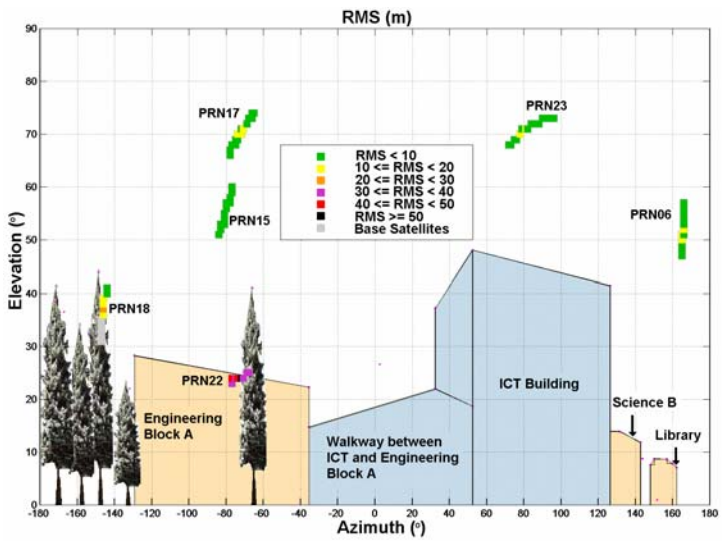

Figure 2: Field RMS Estimated Pseudorange Errors {PRN 22 is behind a building and PRN 18 is masked by coniferous trees}

As an improvement to the initial simulation model, an antenna gain pattern model based on the NovAtel 600 antenna specifications, and used at the remote receiver, was applied to the simulator signals. This gain pattern is shown in Figure 3 and provides more representative simulator C/N_0 values.

Figure 3: Simulator Antenna Gain Pattern – Outdoor Test

In the initial implementation of the simulator model, it was found that the fading effects and pseudorange multipath lacked the stochastic properties required, especially in magnitude, to represent the actual effects observed on PRN 22 and PRN 18. The new multipath model implemented in the GSS 6560 generates fading and error trends due to the addition of phase rates of the echo channels with respect to the LOS channels. The simulation model parameters were selected by trial and error, taking into account the Rician and Rayleigh parameter values estimated by Ma et al (2001), Klukas et al (2003) and Jahn (2001), in order to match the field fading and pseudorange error stochastic properties. The values chosen for the simulation are shown in Figure 4.

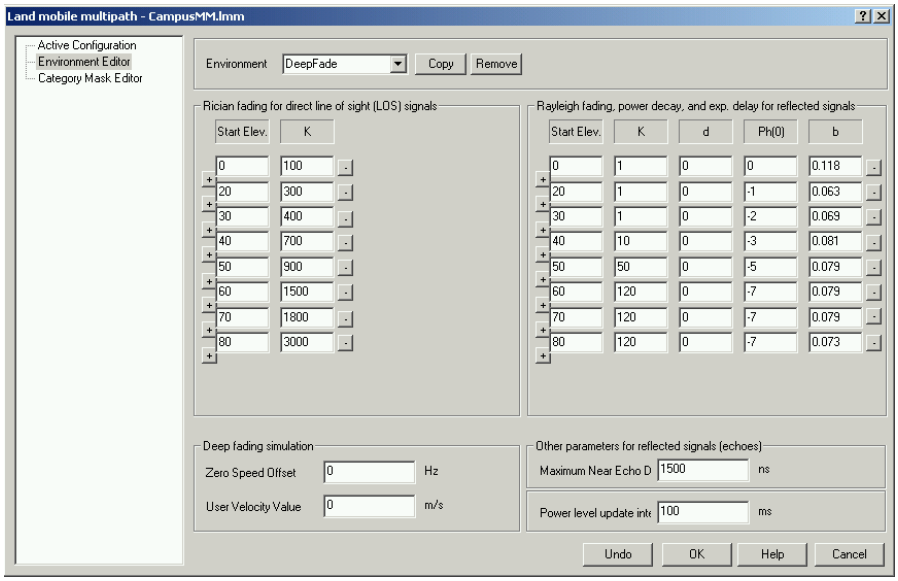

Figure 4: GSS 6560 Model Parameters Used – Outdoor Test

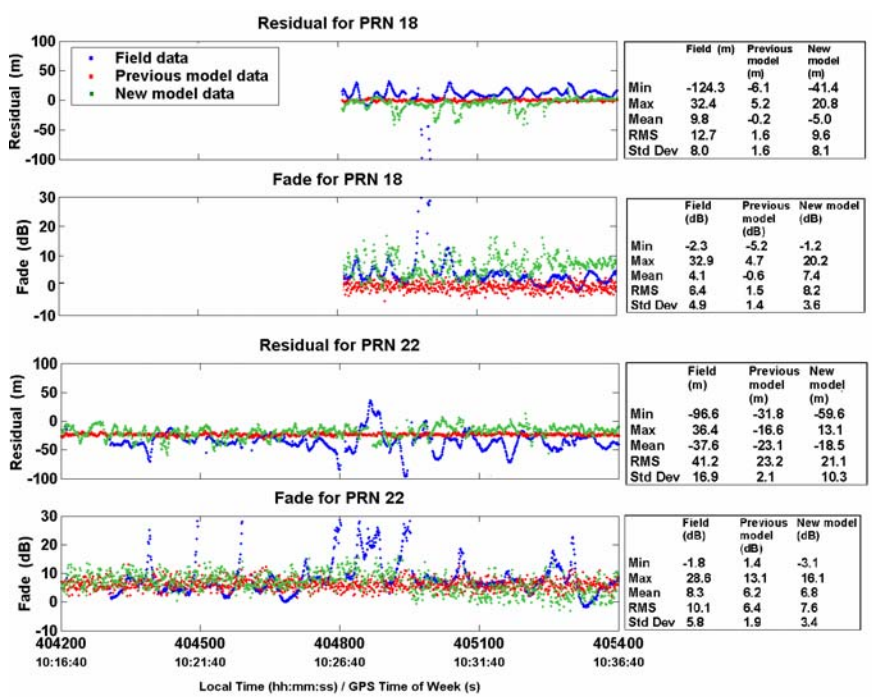

Figure 5: Comparison of Field Measurements and Fixed and Variable Delay Simulation Methods – Outdoor Shaded Signal Environment

As a comparison of the field data with the new variable delay model and with the initial fixed delay model used in Boulton et al (2002), the pseudorange error and signal fading time series and associated statistics for PRN 18 and PRN 22, the satellites of primary interest, are shown in Figure 5. The new model is able to provide deep fading and error trends, which are stochastically more representative of the field data than the previous model. The fading and pseudorange error magnitudes match relatively well for PRN 18. In the case of PRN 22 however, the deep fades of up to 30 dB and multipath caused by echo-only signals still cannot be reproduced. Pseudorange measurements on such faded signals are however very unreliable at best with current receiver tracking technology. It will be shown below that PRN 22 measurements were consistently rejected from the least-squares solutions. The pseudorange error and signal fading statistics for the other simulated satellites, not shown in Figure 5, also matched the field data well. These satellites are generally LOS signals with some multipath errors.

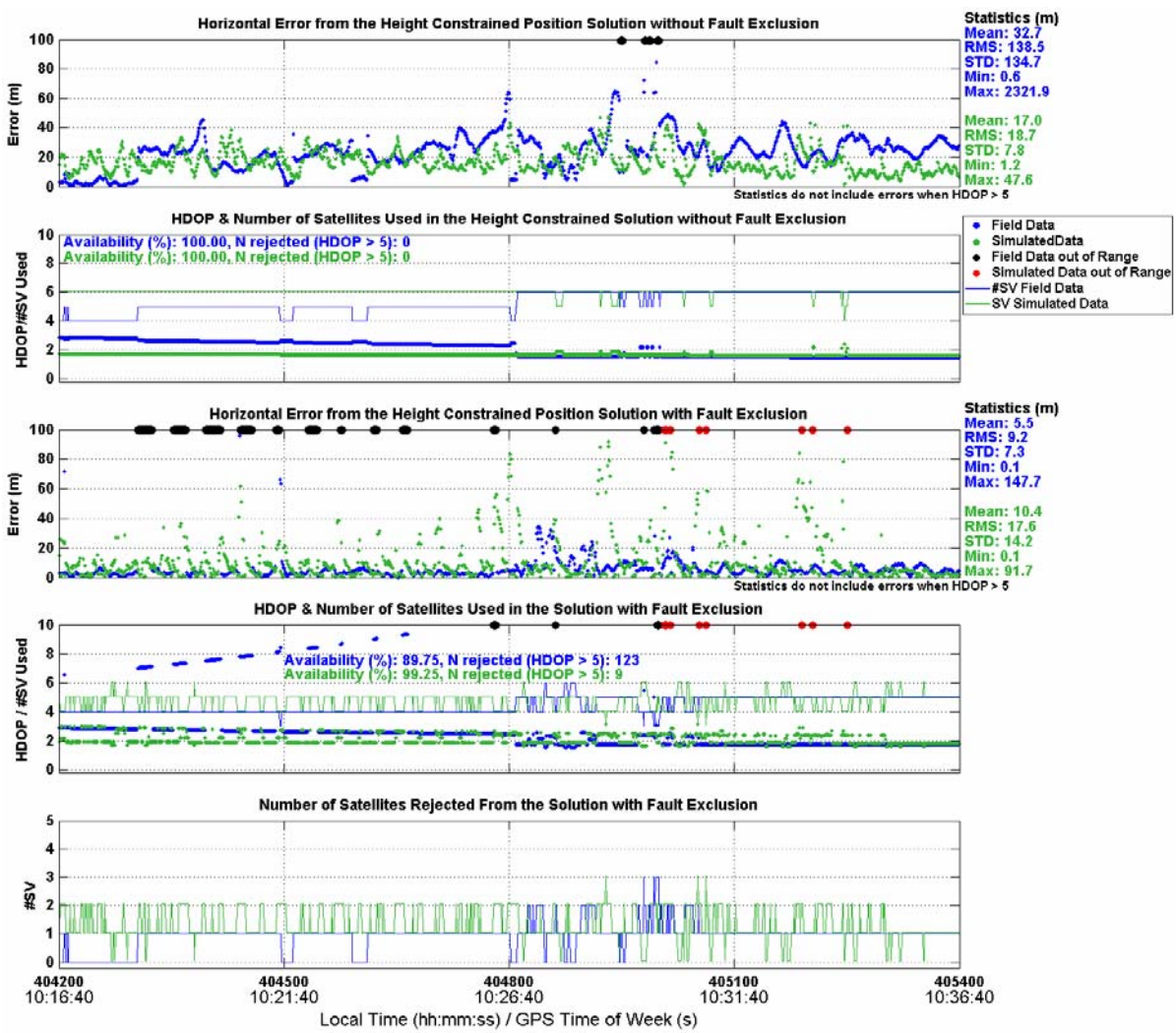

Figure 6: Field and Simulator Horizontal Position Solutions – Outdoor Shaded Signal Environment

Horizontal positions from the field and simulator data were estimated using an epoch-by-epoch least-squares estimation procedure to show clearly the effect of measurement errors at each epoch without any filtering effect. Only the six satellites selected above were used in each case. A cut-off elevation angle of 15 degrees was used. The height was held fixed because it can often be obtained from an external source and a degree of freedom is gained in the process. In order to show the effect of faded measurements on position accuracy, the data was processed twice. In

one case, no measurement fault detection and exclusion process was enabled. In the other case, a 3-sigma rejection criterion was used to reject faulty measurements. The University of Calgary's C^3NAVG^2™ software was use to process and analyse the data. The results of both estimation methods are shown in Figure 6. A position is assumed available when the HDOP ≤ 5. The HDOP was consistently good throughout the test period, with values generally less than 4.0. Availability when no fault detection and exclusion scheme was implemented was 100% for both the field and simulator data. Availability dropped to 90% and 99% for the field and simulator data, respectively, with the fault detection and exclusion scheme implemented. The field position error reached nearly 2.3 km when no fault detection and exclusion scheme was enabled. The corresponding RMS position accuracy was 138 m for the test period in this case. When the fault detection and exclusion scheme was enabled however, the maximum error dropped to 147 m and the corresponding RMS error for the test period to 9 m. The PRN 22 field measurements are excluded most of the time and the PRN 19 measurements some of the time, as expected due to the combination of high noise and multipath. A consequence of exclusion is a HDOP aobve the threshold and lower availability. Although the simulator results have a significantly higher availability, however the RMS accuracy can be considered similar at 17 m. According to this measure, it would appear that this field case was successfully reproduced using the simulator. Figure 7 shows the above results as a function of HDOP in a horizontal map view format.

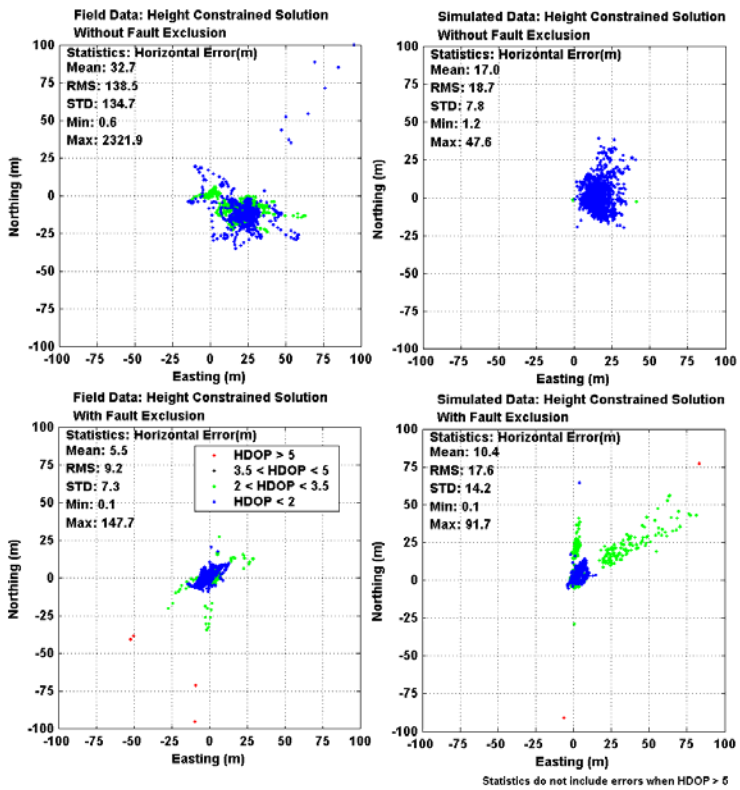

Figure 7: Plan View Position Results - Outdoor Shaded Signal Environment

5 Indoor Results

GPS data was collected inside the upstairs part of a two-storey house shown in Figure 8. The house is of typical wood frame construction with a stucco exterior. However, the roof of the structure is covered with metal shingles, which is not typical of residential dwellings in Calgary. The arrow in Figure 8 indicates the approximate location of the antenna inside the house. The same equipment and differential set-up as described previously was used. A continuous 20-hour data set was recorded.

Figure 8: House used for Indoor GPS Test

The surroundings of the GPS antenna inside the house are shown in Figure 9. Note that three of the four walls of this room are interior walls - other rooms are found on the other side of these walls. The fourth wall is an exterior wall containing the window seen in Figure 9a and the door visible in Figure 9b. Above the room is a standard wallboard ceiling and the metal roof over the attic.

(a) Viewing 160° Azimuth (b) Viewing 45° Azimuth

Figure 9: GPS Antenna Surroundings

Figure 10 show the azimuth and elevation of the six satellites that were simulated for a 20-minute period against the house structural parts obstructing the LOS signals. The same data reduction and analysis procedure and software as used in the previous case were applied here. The 20-minute period selected for simulation on the GPS 6560 is representative of the 20-hour data collected by the receivers.

Using the information show in Figure 10, the multipath category mask for the indoor point was set to that shown in Figure 11. The Category C area roughly corresponds to the exterior wall, although it was extended to an elevation of 40˚, which is higher than the actual wall. According to this mask, LOS signals are only expected from satellites whose LOS propagation paths pass through or near the exterior wall of the room, namely PRNs 26 and 29. No LOS signals are expected through the interior walls or the metal roof above due to a high level of fading. Echoes are anticipated from all satellites except for those below 5°. Given the elevation and azimuth angles of the six satellites of interest and the category mask shown in Figure 11, PRNs 3, 6, 17 and 18 were categorized as Category D (echoes only) whereas PRNS 26 and 29 were categorized as Category C (LOS and echoes).

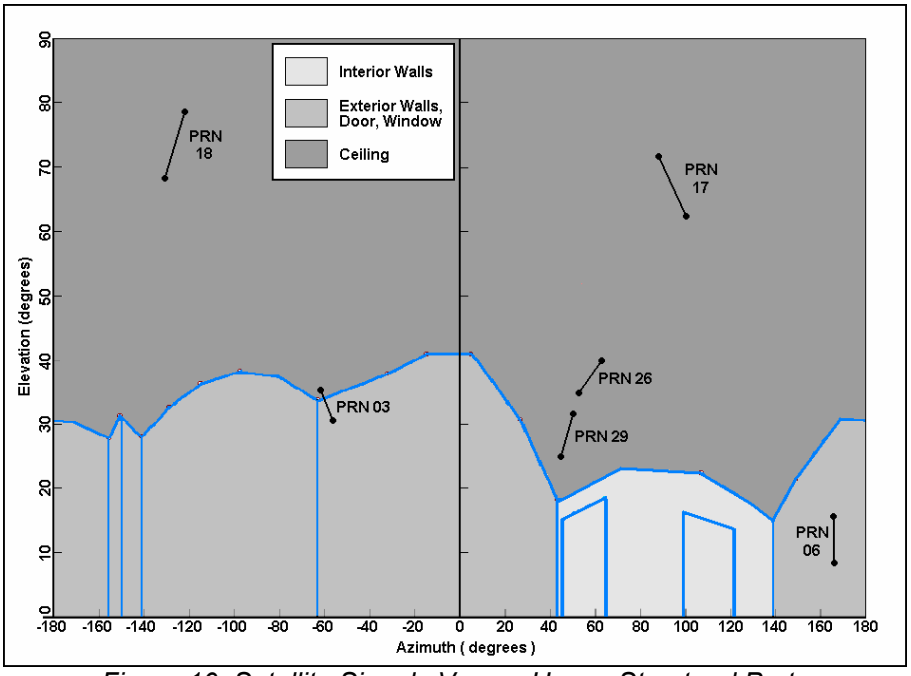

Figure 10: Satellite Signals Versus House Structural Parts

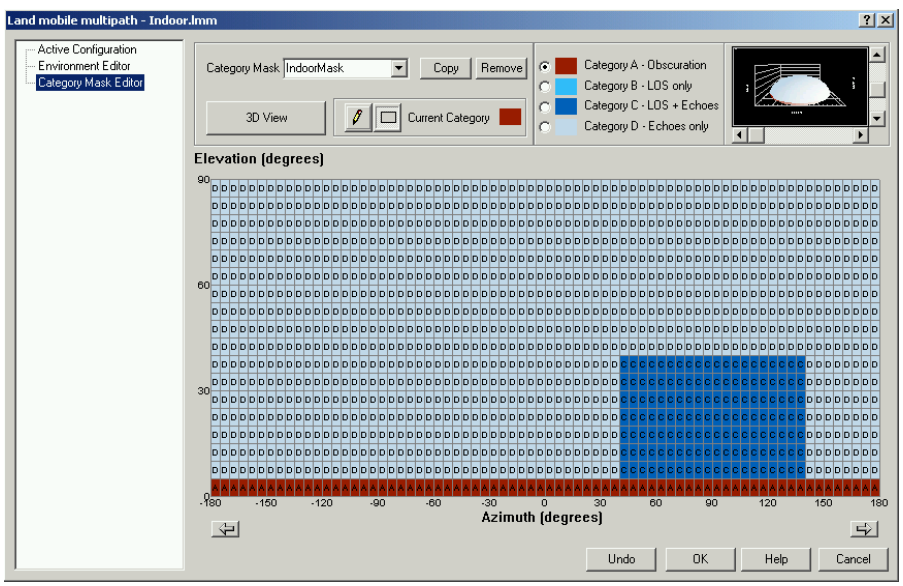

Figure 11: Multipath Category Mask Editor - Indoor Test

The Rician and Rayleigh model parameters were significantly modified from those used for outdoor testing. Signals propagating through a building are likely to reach the antenna via multiple echo paths and possibly also a direct path. Because of strong near echoes, the power of echo signals may be higher relative to the LOS signal than is typically encountered outdoors. Existing simulator parameter sets do not account for the situation in which there is no dominant LOS signal. Therefore the parameters were set primarily through trial and error to create a signal distribution with relatively strong and stable echoes. The parameter values shown in Figure 12 are unusual for this simulator model. However the large *K* and *Ph(0)* values were required to obtain the desired signal set with echo power levels within a few dB of any LOS signals.

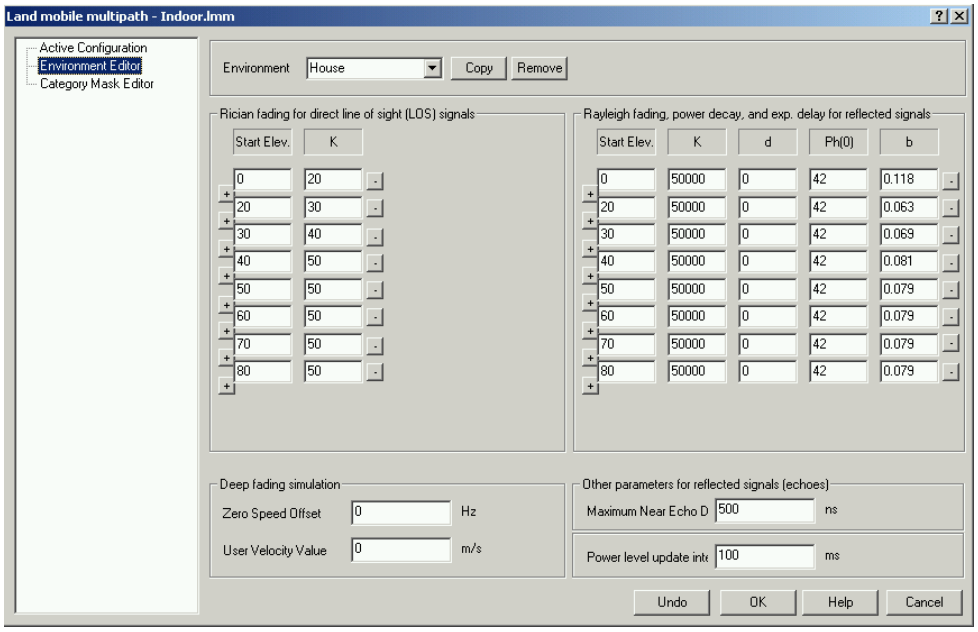

Figure 12: Simulator Model Parameters Used - Indoor Test

As in the case of the outdoor simulation scenario, the antenna gain pattern feature of the simulator was used on the simulated reference station to ensure that simulator C/N_o values were comparable to values obtained in the field. In contrast to the outdoor work, however, the antenna gain pattern was then modified further for the indoor receiver to account for the mean attenuation caused by the building. The gain pattern for the indoor antenna, shown in Figure 13, incorporates the base NovAtel 600 antenna gain pattern in Figure 3 but adds significant attenuation at higher elevations to account for the effects of the metal roof and other surroundings. The gain pattern used is not dependent upon azimuth, although it could be made that way to account for non-isotropic attenuation effects caused by the building structure.

Figure 13: Simulator Antenna Gain Pattern - Indoor Test

In order to better compare to the simulator results, the field data was restricted to the same six satellites as simulated, although additional satellites were tracked. The field C/N_o at the reference site was stable for all six satellites and ranged between 35 and 45 dB-Hz, depending on the satellite. The agreement between field and simulator C/N_o values was within 3 dB for all six satellites. For the indoor point, the field and simulator C/N_o values for all six satellites are shown in Figure 14. Although similar, the C/N_o values measured on the simulator signals are in general

slightly higher than those measured on the field data. The largest discrepancies between the field and simulator C/N_o values occur for PRNs 3 and 18. Note that the field C/N_o values for PRNs 3 and 18 are generally lower than those of the other satellites. From Figure 10 it can be seen that the signals (LOS and echoes) from these two satellites must travel through numerous walls and the portion of the house opposite the exterior wall of the room in which the antenna was located. A similar difference in terms of the simulator C/N_o values cannot be seen. Since the simulator indoor antenna gain pattern is made isotropic (Figure 13), the simulator C/N_o values for PRNs 3 and 18 are similar to those of the other satellites.

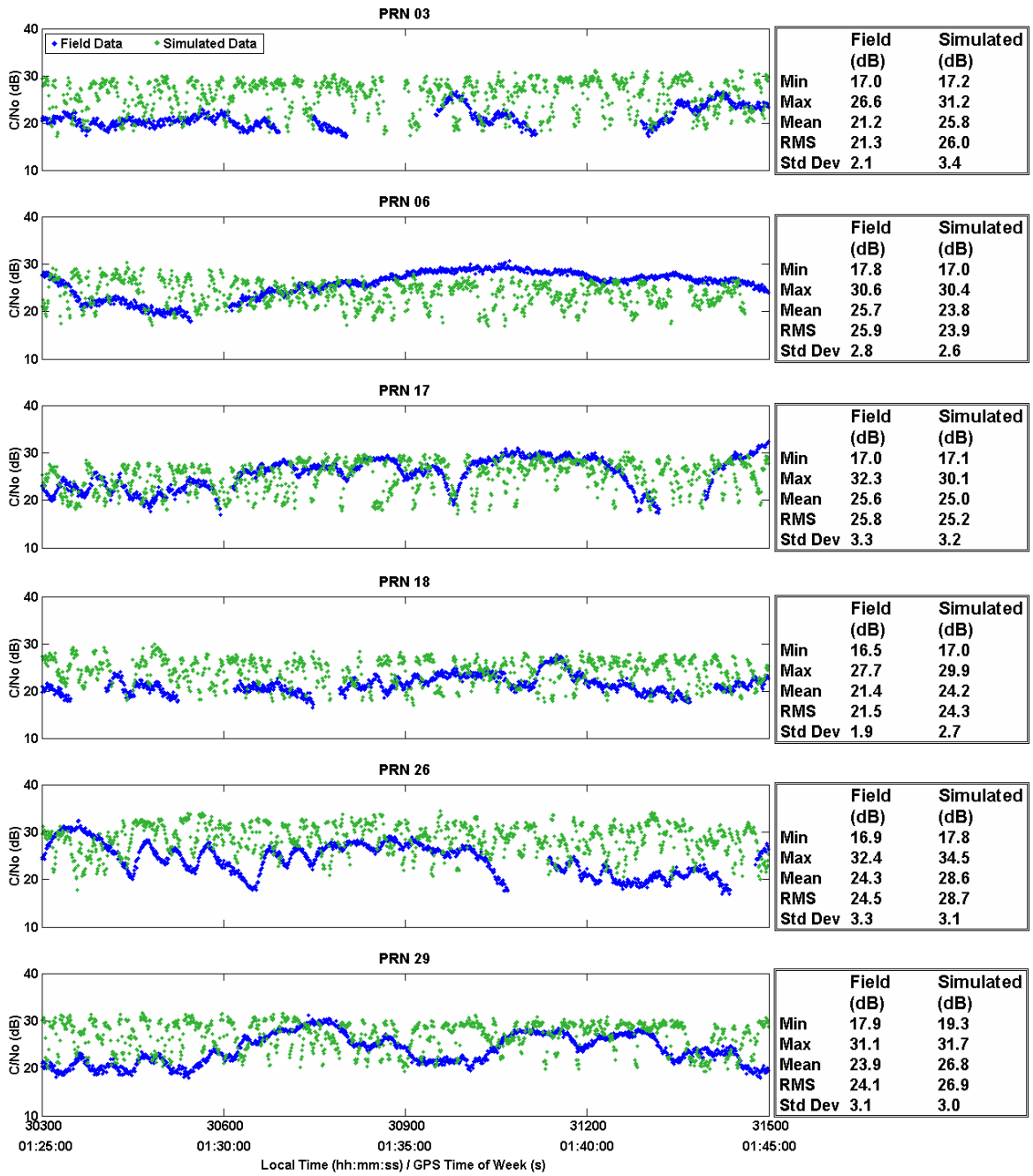

Figure 14: Measured C/N_o - Indoor Test

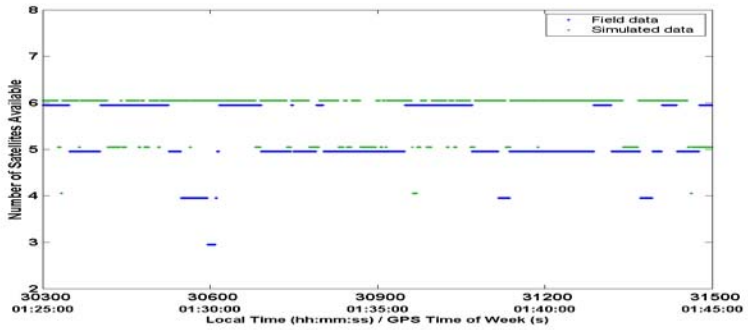

Figure 15 Field and Simulator Satellite Availability

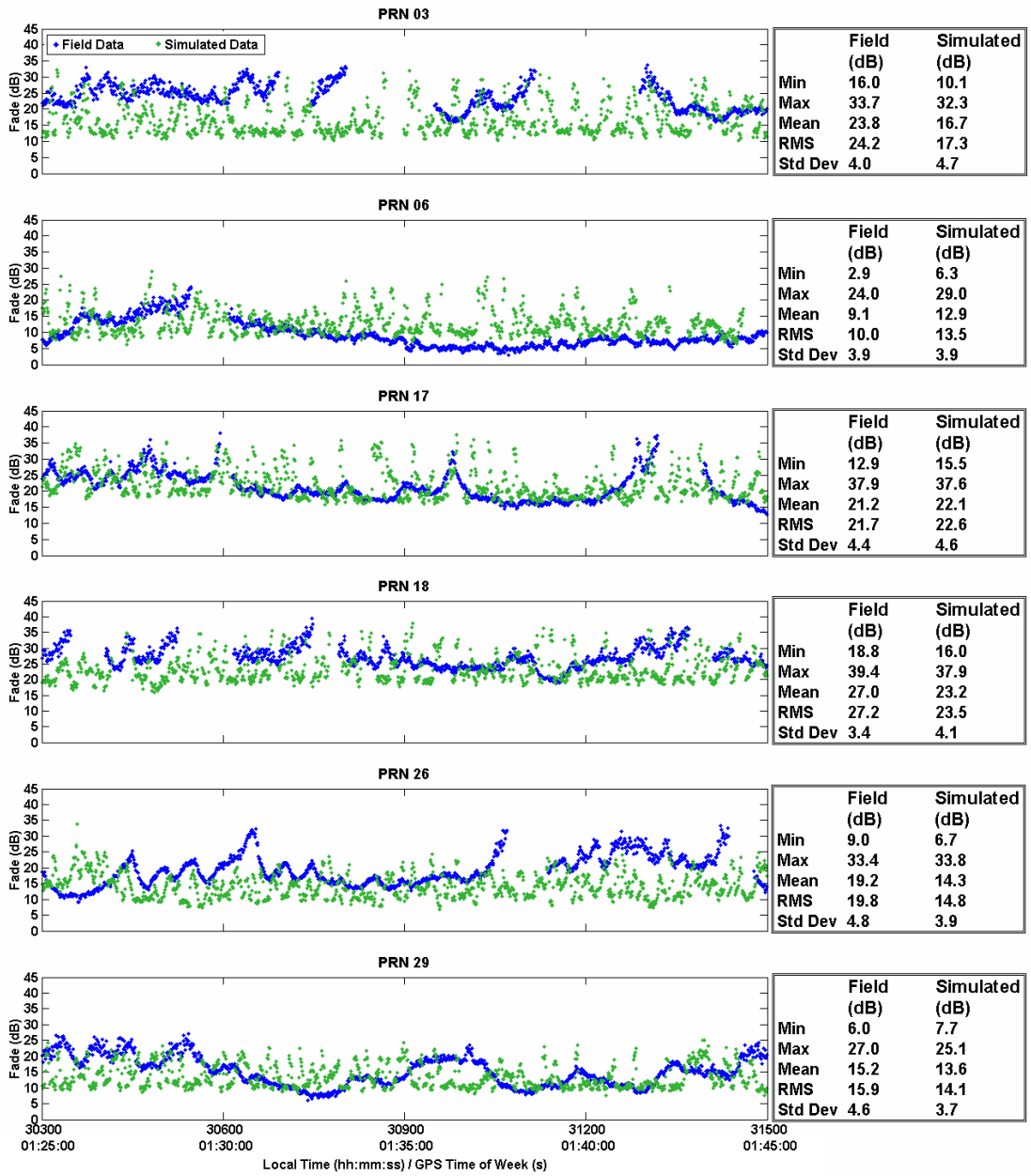

Figure 16: Field and Simulator Fade Values – Indoor Test

With the simulated C/No of Figure 14, satellite tracking availability is generally higher than for the corresponding field data during the 20 minutes of data, as shown in Figure 15. This is partly due to the slightly higher mean C/No, and the more consistent stochastic behaviour of the simulated signals over the test period. The mean number of satellites tracked on the simulator was 5.8, as compared with 5.2 for the field test (based on the set of six satellites selected). The correspondence between field and simulated C/No may be improved with further modifications to the antenna gain pattern of Figure 13, especially through the use of an azimuthally varying pattern. The field and simulator fade values and pertaining statistics for each of the six satellites are shown in Figure 16. In order to achieve simulator fade values for SV 26 and 29 that are of the same order of magnitude as the field fade values, the power of the simulator LOS signal for these two satellites was reduced to a level similar to that of the echoes. This was accomplished through the use of the category mask and Rician and Rayleigh model parameters as discussed earlier. The results of Figure 16 show that the simulator measurements match the field data very well in terms of minimum, maximum and RMS fade values. However, field data variations appear to be of lower frequency than those of the simulator data. This is also seen in the C/N_o values shown in Figure 14.

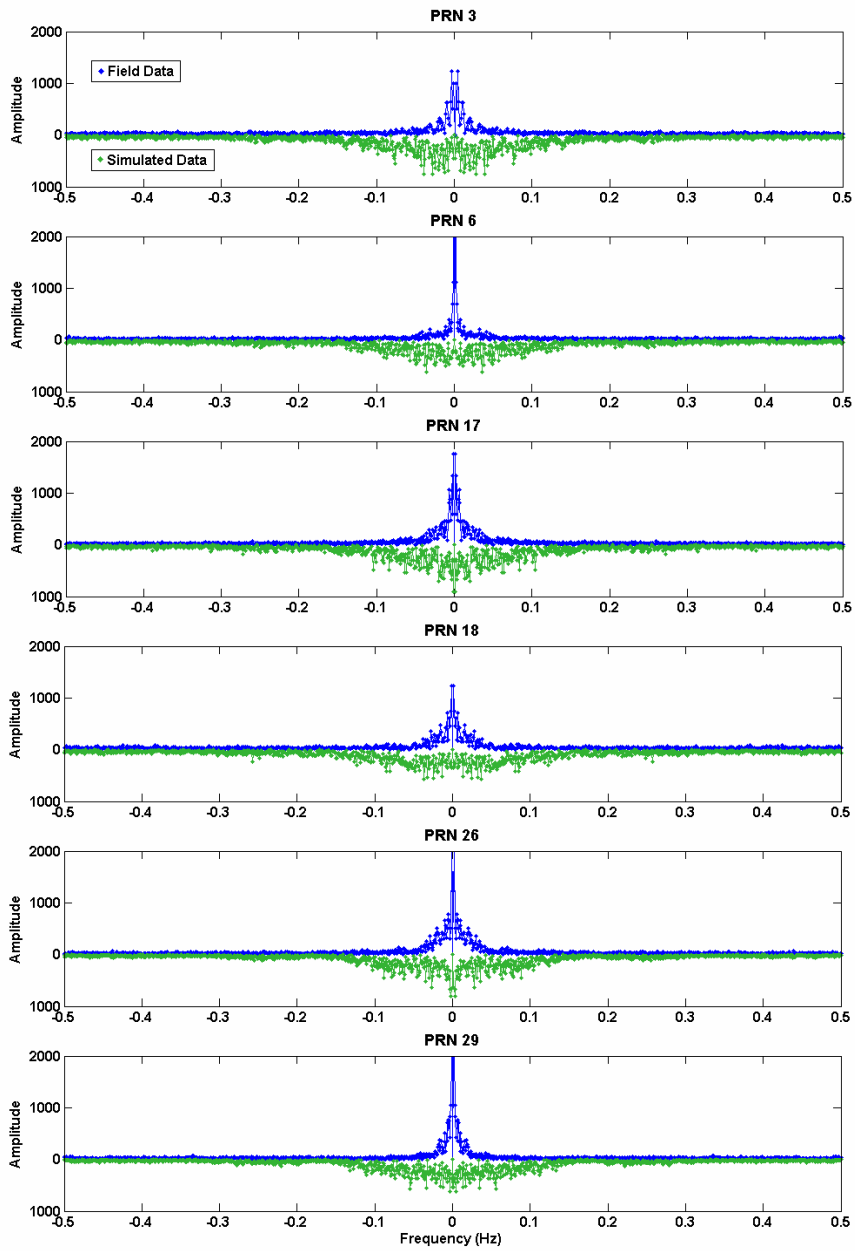

Figure 17: Amplitude Spectra of Field and Simulator Fade Data

The relative fade data spectra are shown in Figure 17. Note that the simulator spectra are shown inverted to aid in the comparison with the field spectra. The agreement is generally good except for low frequencies. The amplitude spectra confirm that for all satellites, the simulator fade data contains more high-frequency components than the field data. Results from a spectral analysis of absolute C/N_o lead to the same conclusion. One possibility is that the rate of change in path length of the signals is changing more quickly in simulation than in the field test. This would result in a faster fading rate, as seen in the simulator results of Figure 16.

The position-constrained epoch-by-epoch residuals from both the field data and simulator data are shown in Figure 18. Since the position is constrained, these residuals constitute a direct measure of the pseudorange errors. The agreement between the field and simulation is very good, especially for PRNs 3, 17 and 18. The largest discrepancy exists for PRN 6 in which case the simulator data produces a large bias and standard deviation in the residuals. Given the position of PRN 6 (see Figure 10), it is possible that in practice, a direct signal was actually present which could have been classified as LOS in the simulator. The corresponding measured C/N_o and fade values support this suggestion. Note that the measured C/N_o for this satellite, as seen in Figure 14, is relatively high (30 dB-Hz) for much of the 20-minute test compared to the other satellites. This is not the case for the simulator C/N_o. Consequently, the simulator residuals for PRN 6 are pessimistic in terms of a large bias caused by the lack of a LOS component, and a large standard deviation due to a lower and less stable C/N_o. This example demonstrates the importance of correctly categorizing each satellite with the Category Mask Editor.

The amplitude spectra of the residuals for the field and simulator data, not shown here, are even more consistent than either the fade or absolute C/N_o spectra.

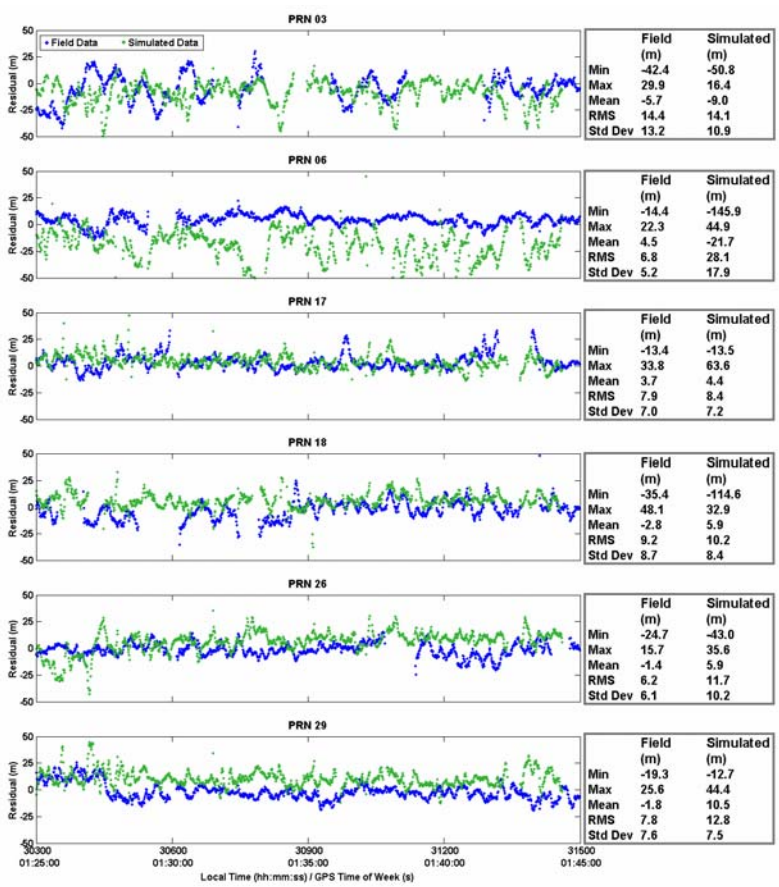

Figure 18: Field and Simulator Position-Constrained Residuals - Indoor Test

Finally, the position results are shown in Figures 19 and 20. These figures report the same type of results as shown in Figures 6 and 7 for the outdoor test. As in the case of the outdoor test, only the six satellites used by the simulator were included in the field data solution in order to have the same geometry and redundancy. Availability (HDOP ≤ 5) is always higher than 94%, which is remarkable for a complete indoor case. The field and simulator results are generally in very good agreement, once more confirming the effectiveness of the overall simulator scenario used. The solutions based on the fault detection and exclusion scheme results in slightly higher RMS values. This is not unusual, given that no extraordinary large faults were present to start with and that the measurements that were excluded weakened the geometry resulting in slightly large errors in some cases. However this is not a valid reason to use solutions without any fault detection and exclusion if a reasonable level of reliability is to be maintained.

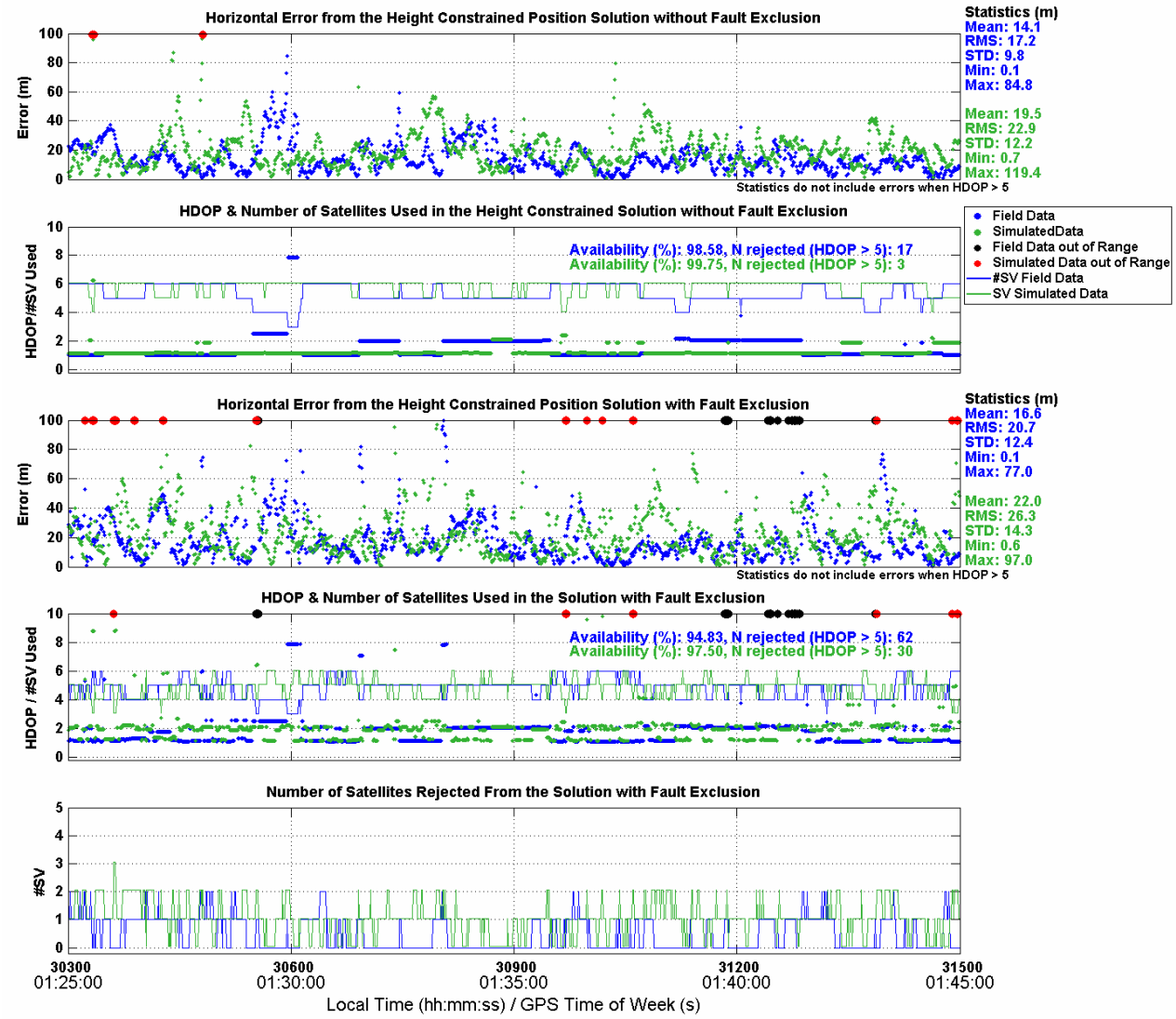

Figure 19: Field and Simulator Horizontal Position Solutions – Indoor Test

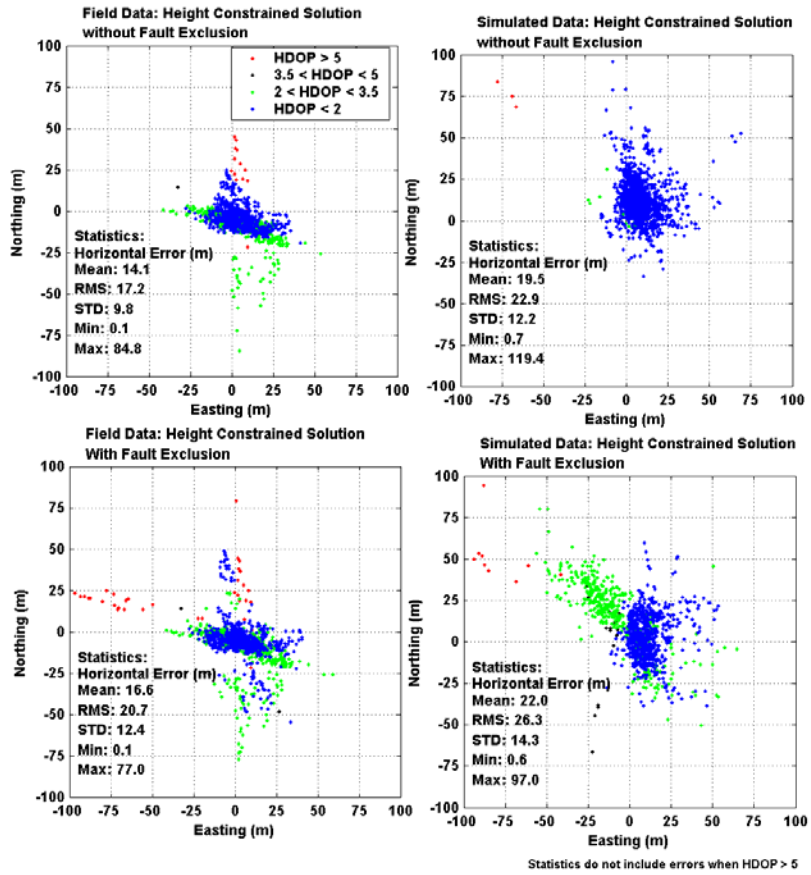

Figure 20: Plan View Position Results – Indoor Test

It is worth noting that the full 2-hour field data set was also processed to assess overall performance. 2-D position availability was of the order of 98% and the RMS, of the order of 20 m. This shows that GPS indoor signal tracking functions well inside typical North American residences.

6 Conclusions

The results reported herein show that, at least for the two environments tested, the hardware simulator used, namely the GSS 6560, is capable of reproducing the fade and multipath environment with sufficient fidelity to test a receiver under a totally controlled environment, at least as a first approximation. Other improvements in the simulator models are possible. Since to some extent the changes to the multipath model add a geometrical relationship rather than remaining purely statistical, other aspects of the overall model may need to be reviewed. For example, the initial delay, δ_i, is specified by an exponential distribution, which probably already includes the effect of variation in reflection angle, and the use of satellite elevation and azimuth may be changing the shape of this distribution. It may be appropriate to continue the extension of the model and define a randomly generated initial value for D, thus making the process more empirical. The test for this would be whether the resulting simulation yielded the same stochastic characteristics as that observed in the real-world cases.

In terms of future testing, another type of HSGPS receiver will be used to confirm that the simulator scenarios still agree reasonably well with the field data, even when different correlation and other signal processing schemes are used in the receiver. In addition, the testing of different antennas, more suitable for personal use, is required. More refined non-isotropic horizontal antenna patterns will be tested to improve the agreement between field and simulator values. A lower base level for the received satellite power will be used in the simulator, because the default power level is probably 3 dB higher than that of current satellites. This could explain why the

simulator C/N_o values tend to be higher. The tests reported herein were conducted in static mode. Although early results suggest that the HS receiver used is not affected by regular personal motion, further dynamic characterization is required. An epoch-by-epoch least-squares approach was deliberately used here to assess signal performance. This is sub-optimal for actual field use in which case a Kalman filter and integration with self-contained sensors would obviously improve position performance (e.g. Mezentsev et al 2002, Stirling et al 2003).

References

Boulton, P, A. Read, G. MacGougan, R. Klukas, E. Cannon, and G. Lachapelle (2002), Proposed Models and Methodologies for Verification Testing of AGPS-Equipped Cellular Mobile Phones in the Laboratory, Proceedings of the GPS-02 Conference (Portland, September 24-27), U.S. Institute of Navigation, 200-212.

Cannon, M.E., G. Lachapelle, G. MacGougan, R. Klukas, P. Boulton, and A. Read (2003) Weak Signal Environment Testing of a High Sensitivity GPS Receiver in the Laboratory. GPS World, 14, 3 (March), 24-32.

Garin, L. J., M. Chansarkar, S. Miocinovic, C. Norman, and D. Hilgenberg (1999) Wireless Assisted GPS-SiRF Architecture and Field Test Results. Proceedings of the Institute of Navigation ION GPS-99 (September 14-17,1999, Nashville, Tennessee), 489–497.

Jahn, A. (2001) Propagation Considerations and Fading Countermeasures for Mobile Multipmedia Services. International Journal of Satellite Communications, 19, 223-250.

Klukas, R., G. Lachapelle, C. Ma, and G. Jee (2003) A GPS Signal Fading Model for Urban Centres. IEE Proceedings of Microwaves, Antennas and Propagation, in press.

Ma, C., G. Jee, G. MacGougan, G. Lachapelle, S. Bloebaum, G. Cox, L. Garing and J. Shewfelt (2001) GPS Signal Degradation Modeling. Proceedings of GPS2001, (Session C2, Salt Lake City, September 11-14), The Institute of Navigation, Alexandria, VA, pp. 882-893.

MacGougan, G. (2003) High Sensitivity GPS Performance Analysis in Degraded Signal Environments. MSc Thesis, Department of Geomatics Engineering, University of Calgary, in preparation.

MacGougan, G., G. Lachapelle, R. Klukas, K. Siu, L. Garin, J. Shewfelt, and G. Cox (2002) Performance Analysis of A Stand-Alone High Sensitivity Receiver. GPS Solutions, Springer Verlag, 6, 3, 179-195.

Mezentsev, O., Y. Lu, G. Lachapelle, and R. Klukas(2002) Vehicular Navigation in Urban Canyons Using a High Sensitivity Receiver Augmented with a Low Cost Sensor. Proceedings of GPS2002 (Session E1, Portland, OR, 24-27 September), The Institute of Navigation, Alexandria, VA, 363-369.

Stirling, R., J. Colllin, K. Fyfe and G. Lachapelle (2003) An Innovative Shoe-Mounted Pedestrian Navigation System. Proceedings of GNSS 2003, The European navigation Conference (Graz, Austria, 22-25 April).

Acknowledgements

The authors acknowledge the assistance of Mr. Glenn MacGougan in reducing and analyzing the data.